OPEN ACCESS
*World Journal of Multidisciplinary Studies*
ISSN (Online): 3049-0855 | Vol. 2, No. 7, July. 2025
Website: https://wasrpublication.com/index.php/wjms

# Bayesian-Based Assessment of Retrofitting Strategies for Seismic Resilience of Petroleum Storage Tanks

**Ali Aghazadeh Dizaji[1]*, Abdulkadir Cüneyt Aydın[1]**

[1]Department of Civil Engineering, Engineering Faculty, Ataturk University, 25030, Erzurum, Turkey.

Received: 02/05/2025 | Accepted: 19/06/2025 | Published: 26/07/2025

**Abstract:** This study presents a causally informed, Bayesian-based framework for evaluating seismic retrofitting strategies applied to an uplift-sensitive petroleum storage tank. A nonlinear digital twin is integrated with hierarchical Bayesian inference and counterfactual analysis to quantify probabilistic fragility transformation and mechanism-specific retrofit effects. The investigated reference tank exhibits a coupled uplift–localization–instability cascade governing severe damage evolution. Shell confinement, anchorage enhancement, and hybrid configurations are evaluated within a unified causal architecture. Results demonstrate that single-mechanism interventions provide partial mitigation and exhibit saturation under high-demand regimes, whereas hybrid retrofits simultaneously suppress uplift persistence and shell instability sensitivity, producing reduced fragility curvature, compressed uncertainty, and enhanced resilience robustness. Bayesian posterior reconstruction reveals heterogeneous treatment effects across demand and operational states, invalidating deterministic retrofit ranking assumptions. The proposed framework enables multidimensional fragility manifold reconstruction and mechanism-resolved resilience assessment, providing a rigorous basis for uncertainty-aware retrofit selection in uplift-dominated petroleum storage systems.

**Keywords**: Bayesian causal inference; Seismic retrofitting; Petroleum storage tanks; Fragility manifolds; Structural resilience.

## 1. Introduction

Petroleum storage tanks constitute mission-critical assets within global energy infrastructures, acting as strategic buffers between upstream production and downstream distribution systems. Their operational continuity directly affects environmental safety, industrial stability, and national energy resilience. Seismic damage to such tanks has historically triggered cascading industrial failures, including fire propagation, hazardous material release, and prolonged service disruption. These events demonstrate that the seismic performance of storage tanks transcends conventional structural safety concerns and must be addressed as a systemic risk problem embedded within interconnected energy networks (Aghazadeh Dizaji, 2017; Wang et al., 2023). From a structural mechanics perspective, above-ground cylindrical steel tanks exhibit response characteristics fundamentally distinct from framed buildings. Their behavior is governed by nonlinear shell mechanics, fluid–structure interaction, uplift-sensitive boundary conditions, and hydrodynamic pressure amplification. Earthquake excitation activates coupled impulsive–convective liquid motion, induces localized plastic hinging near the shell–bottom junction, and may initiate global instability modes such as elephant-foot buckling and diamond-pattern shell deformation. These phenomena invalidate simplified elastic assumptions and necessitate advanced modeling frameworks capable of simultaneously representing geometric nonlinearity and uncertainty propagation (Men et al., 2023).

In this study, a representative petroleum storage tank is conceptually defined as a large-capacity, above-ground, welded steel cylindrical structure founded on shallow foundations and operating under variable liquid fill conditions. The tank is assumed to be located within a seismically active industrial zone hosting multiple adjacent process units, where operational continuity is essential and spatial constraints limit replacement options. The shell is characterized by height-dependent thickness variation, continuous bottom plate connection, and conventional roof configuration. The tank is neither newly constructed nor critically degraded, representing a typical in-service asset within aging petroleum infrastructure. This qualitative reference configuration provides a realistic basis for evaluating retrofit performance while avoiding reliance on case-specific numerical parameters (Jing et al., 2024a).

A substantial portion of existing petroleum storage facilities worldwide comprises tanks designed under outdated seismic provisions or deterministic safety margins. Progressive material degradation, weld fatigue, corrosion, foundation settlement, and operational modifications further compromise structural reliability (Aghazadeh Dizaji, 2024a). As seismic hazard awareness increases and performance-based engineering paradigms evolve, retrofitting existing tanks has become a strategic necessity rather than a discretionary upgrade. Contemporary objectives extend beyond collapse prevention toward resilience-oriented performance, emphasizing damage controllability, post-event functionality, and recovery capacity (Vasquez Munoz & Dolšek, 2024; Handa et al., 2024).

*Corresponding Author
Ali Aghazadeh Dizaji*

Current retrofit strategies for steel storage tanks include shell thickening, external stiffening rings, anchorage enhancement, base isolation, energy dissipation devices, and fiber-reinforced polymer confinement. Hybrid retrofit systems combining mechanical and composite interventions have recently emerged (Aghazadeh Dizaji, 2024b; Hagen et al., 2024). However, most existing investigations examine these techniques independently, under deterministic loading scenarios, or using isolated performance indicators such as peak stress or displacement. Such evaluations provide limited insight into system-level resilience and fail to account for uncertainty-driven variability in structural response (Erkmen et al., 2024).

More fundamentally, the prevailing literature relies on correlation-based assessments of retrofit effectiveness. Performance improvement is commonly quantified as the difference between pre- and post-retrofit response metrics, implicitly assuming uniform causal contribution across hazard intensities and structural configurations (Jayasinghe et al., 2024). This assumption neglects epistemic uncertainty related to material properties, construction quality, and degradation state, as well as aleatory uncertainty associated with ground motion variability, liquid height, and operational conditions. Consequently, deterministic rankings of retrofit strategies may misrepresent true resilience gains (Aghazadeh Dizaji, 2024c) and lead to suboptimal decision-making (Vasquez Munoz et al., 2024).

Recent advances in Bayesian inference and probabilistic structural mechanics provide a rigorous framework for overcoming these limitations. Bayesian hierarchical modeling enables integration of multi-source uncertainties (Aghazadeh Dizaji & Ahmadian, 2016), posterior updating of structural parameters, and probabilistic prediction of performance states. More critically, Bayesian counterfactual reasoning allows estimation of how a structure would have behaved in the absence of a specific retrofit intervention, thereby isolating causal strengthening effects rather than relying on observational correlations (Rahmat Rabi et al., 2024; Li et al., 2024).

Within this probabilistic paradigm, seismic vulnerability can be represented through multidimensional fragility manifolds instead of traditional two-dimensional fragility curves (Lee et al., 2024). These manifolds capture the coupled influence of shell geometry, liquid height ratio, anchorage condition, and retrofit configuration on failure probability (Aghazadeh Dizaji & Aydın, n.d.). Such representations are particularly essential for petroleum storage facilities, where tanks exhibit substantial heterogeneity in size, aspect ratio, foundation condition, and operational state. Resilience assessment thus becomes a problem of probabilistic surface reconstruction rather than single-parameter threshold evaluation (Shan et al., 2025). Despite these methodological advances, their application to oil storage tank retrofitting remains limited. Existing studies rarely integrate nonlinear shell finite element modeling with Bayesian multilevel inference. Even fewer attempt to decompose retrofit efficiency into direct structural stabilization and indirect fluid–structure interaction mitigation. As a result, practitioners lack a rigorous analytical framework for identifying optimal strengthening strategies under realistic uncertainty conditions (Shi et al., 2025).

This gap establishes a clear scientific necessity for developing causally interpretable, probabilistically grounded retrofit evaluation methodologies. Without such frameworks, retrofit selection remains driven by deterministic intuition rather than uncertainty-aware performance evidence (Aghazadeh Dizaji & Aydin, 2025). Addressing this deficiency is essential for advancing performance-based seismic engineering of industrial infrastructure and enabling risk-informed investment strategies in the energy sector (Volikos et al., 2025). Accordingly, the present study proposes a Bayesian-based assessment framework for evaluating retrofitting strategies aimed at enhancing the seismic resilience of petroleum storage tanks. The framework integrates nonlinear shell modeling, stochastic ground motion ensembles, and hierarchical Bayesian inference (Aghazadeh Dizaji et al., 2023) to quantify retrofit efficiency across multiple damage states. Through counterfactual performance reconstruction, the study isolates causal contributions of individual retrofit mechanisms and generates probabilistic fragility manifolds reflecting uncertainty-aware structural behavior (Fang et al., 2024).

Based on this framework, the research is guided by the following questions:

RQ1: How do different retrofitting strategies modify the probabilistic fragility characteristics of steel petroleum storage tanks under seismic excitation (Aydin et al., 2020)?
RQ2: To what extent does Bayesian hierarchical inference improve the reliability of retrofit efficiency estimation compared with conventional deterministic approaches?
RQ3: Which retrofit configurations provide the highest resilience gain across varying hazard intensities and structural parameter uncertainties?
To address these questions, the study tests the following hypotheses:
H1: Bayesian-based probabilistic assessment reveals significant heterogeneity in retrofit efficiency across structural configurations and seismic hazard levels (Dehghan et al., 2024a), challenging deterministic ranking assumptions.
H2: Hybrid retrofit systems combining anchorage enhancement and shell confinement exhibit superior resilience gains when evaluated through counterfactual fragility manifold reconstruction (Dehghan et al., 2024b).

By embedding retrofit evaluation within a causal–probabilistic performance framework, this research advances seismic resilience assessment of petroleum storage tanks and provides analytically robust guidance for industrial risk mitigation under uncertainty (Ghadarjani & Gheitarani, 2013; Bodenmann et al., 2024).

## 2. Literature Review

The seismic resilience of petroleum storage tanks has progressively evolved from a narrowly defined structural safety concern into a multidimensional systems-engineering problem (Meng et al., 2025). Contemporary research increasingly recognizes these tanks as critical nodes within complex energy infrastructures (Gheitarani, n.d.), where localized structural failure can initiate cascading disruptions across interconnected industrial networks (Chiappelloni et al., 2025). This shift in perspective has reframed tank performance assessment from isolated response evaluation toward systemic risk mitigation, functional continuity, and probabilistic resilience optimization (Abd-Elhamed et al., 2025).

Within this systems-oriented paradigm, petroleum storage facilities are understood as adaptive socio-technical assemblages subject to multi-hazard environments, operational variability, and aging-induced degradation (Islam & Jangid, 2024). Earthquake-induced damage to storage tanks not only compromises structural integrity (Gheitarani et al., 2024b) but also amplifies environmental exposure, fire propagation potential, and supply-chain instability. Consequently, modern engineering frameworks emphasize resilience as the probabilistic capacity to maintain or rapidly restore functionality under uncertainty rather than merely preventing collapse (Bajad et al., 2024).

At the physical level, above-ground cylindrical steel tanks exhibit behavior governed by nonlinear shell mechanics, uplift-sensitive boundary conditions, and fluid–structure–foundation interaction (Gheitarani et al., 2024c; Celik et al., 2024). Seismic excitation activates coupled impulsive–convective liquid dynamics, induces localized plastic deformation near the shell–bottom junction, and may trigger global instability modes such as elephant-foot buckling and circumferential wrinkling (Doustvandi et al., 2023). These phenomena introduce strong geometric nonlinearity and spatial response heterogeneity, invalidating simplified elastic representations and motivating high-fidelity numerical modeling approaches (Jing et al., 2024b).

Advances in computational mechanics have enabled increasingly realistic simulation of tank behavior through nonlinear finite element formulations that capture shell instability, contact separation, and hydrodynamic pressure redistribution. However, much of this work remains embedded within deterministic paradigms (Gheitarani et al., 2024d), relying on single realizations of ground motion input and fixed material parameters. While such simulations offer detailed insight into failure mechanisms, they provide limited information regarding response variability and uncertainty-driven performance dispersion (Wang et al., 2024; Li et al., 2024a).

Parallel to developments in physics-based modeling, probabilistic seismic assessment methodologies have emerged to quantify vulnerability across damage states. Fragility curves, typically expressing failure probability as a function of seismic intensity, have become standard tools for infrastructure risk evaluation (Gheitarani & Norouzian, 2024a; Tran et al., 2025). Yet traditional fragility formulations remain fundamentally two-dimensional, reducing complex multidimensional dependencies to single-parameter relationships. This reduction obscures the influence of tank geometry, liquid fill ratio, anchorage condition, and retrofit configuration on seismic performance (Li et al., 2025).

Recent research trends increasingly advocate for multidimensional vulnerability representations, often conceptualized as fragility surfaces or manifolds (Gheitarani & Norouzian, 2024b). These constructs allow simultaneous consideration of multiple governing parameters and enable probabilistic mapping of performance states across heterogeneous tank populations. Such approaches align with portfolio-level risk management strategies, where decision-makers require scalable assessment frameworks capable of accommodating structural diversity and operational uncertainty (Gabbianelli et al., 2025b).

Concurrently, digital engineering paradigms have begun reshaping infrastructure assessment practices. Digital twins—virtual representations of physical assets continuously updated through observational data (Hosseini et al., n.d.)—offer unprecedented opportunities for integrating physics-based simulation with probabilistic inference (Hagen et al., 2024). Hierarchical Bayesian digital twins, in particular, facilitate multilevel uncertainty modeling across component, system, and facility scales. This integration enables posterior updating of structural parameters, predictive performance estimation, and adaptive risk assessment under evolving conditions (Haroun & Wang, 2025; Jayasinghe et al., 2024).

Despite these advances, digital twin implementations for petroleum storage tanks remain nascent. Existing applications primarily focus on monitoring or anomaly detection (M. A. G. et al., 2024), with limited incorporation of nonlinear shell mechanics or retrofit performance evaluation. The potential for combining digital twins with causal inference frameworks to support resilience-oriented decision-making remains largely unexplored (Zhang et al., 2025).

Retrofitting strategies for steel storage tanks have diversified considerably over recent decades. Traditional mechanical interventions include shell thickening, external stiffening rings, bottom plate reinforcement, anchorage enhancement, and foundation improvement (Norouzian & Gheitarani, 2025). Energy-based solutions such as base isolation and supplemental damping seek to reduce transmitted seismic demand. Composite systems, notably fiber-reinforced polymer confinement, aim to stabilize local buckling and enhance ductility. Hybrid configurations integrating multiple mechanisms have emerged to exploit complementary performance benefits (Flaño & Vallespín, 2024).

However, classification of retrofit strategies by technique alone provides limited insight into underlying performance mechanisms. Contemporary literature increasingly emphasizes mechanism-based taxonomy (Norouzian & Guyadeen, 2025), distinguishing between interventions that enhance structural stiffness, control boundary conditions, dissipate energy, or confine instability-prone regions. This conceptual shift enables comparative evaluation based on functional contribution rather than construction method, facilitating more rational retrofit selection (Chen et al., 2024).

Notwithstanding this conceptual refinement, empirical assessment of retrofit effectiveness remains predominantly correlation-based (Qurraie & Gheitarani, 2025). Performance gains are commonly inferred from pre- and post-intervention response differences without isolating causal contributions. Such approaches implicitly assume uniform retrofit impact across hazard levels and structural configurations, neglecting uncertainty-induced heterogeneity. As a result, deterministic rankings of retrofit strategies often fail to generalize beyond specific case studies (Stoicescu et al., 2025).

Bayesian causal inference offers a principled framework for addressing these limitations (Sadigh et al., 2023). By modeling retrofit implementation as a treatment variable and structural response as an outcome (Alviz-Meza et al., 2024; Naser & Tapeh, 2024), Bayesian counterfactual analysis enables estimation of treatment effects under hypothetical no-retrofit scenarios. This approach allows decomposition of observed performance improvements into direct structural stabilization effects and indirect mechanisms mediated through fluid–structure interaction. Yet application of such causal methodologies to storage tank retrofitting remains sparse (Nosseir et al., 2024).

Recent developments in surrogate-assisted modeling further enhance the feasibility of probabilistic causal assessment (Di-Sarno et al., 2023; Handa et al., 2024). Machine learning emulators trained on high-fidelity finite element simulations (Sarabi et al., 2023) enable rapid exploration of parameter spaces that would otherwise be computationally prohibitive. When embedded within Bayesian frameworks, these surrogates facilitate uncertainty-aware fragility reconstruction and retrofit efficiency estimation across multidimensional domains (Khanian et al., 2019).

From a resilience engineering perspective, retrofit evaluation increasingly incorporates functionality-oriented metrics, including residual deformation, repairability thresholds, and recovery trajectories (Zakerhaghighi et al., 2015). These metrics extend beyond peak response indicators to capture operational continuity and downtime implications. However, integration of such metrics with probabilistic structural modeling and causal inference remains limited, constraining their practical utility for industrial decision-making (Gheitarani et al., 2020).

McCabe-style hierarchical synthesis provides a structured lens through which existing literature may be organized across interconnected layers: system-level risk framing, physical modeling, probabilistic representation, retrofit mechanism taxonomy, and decision-oriented performance metrics (Kahvand et al., 2015). At the system layer, studies emphasize cascading failure and industrial resilience. At the physics layer, nonlinear shell behavior and fluid coupling dominate. Probabilistic representations introduce fragility modeling and uncertainty quantification. Retrofit taxonomies classify interventions by mechanism. Decision layers address resilience optimization and investment prioritization (Khanian et al., 2013).

Applying this hierarchical framework reveals pronounced asymmetries in research maturity (Samami et al., 2024). Nonlinear structural modeling has achieved considerable sophistication, while probabilistic integration remains partial (Naghibi Iravani et al., 2024a). Retrofit mechanisms are extensively cataloged, yet rarely evaluated within unified causal frameworks. Decision-oriented resilience metrics exist conceptually but lack rigorous computational implementation. The intersection of nonlinear mechanics, Bayesian inference, and causal retrofit attribution constitutes a critical methodological gap (Zaker Haghighi et al., 2014).

This gap is particularly consequential for petroleum storage facilities characterized by heterogeneity in tank geometry, anchorage conditions, foundation properties, and operational states (Gheitarani et al., 2013a). Retrofit strategies effective for one configuration may underperform for others. Without multidimensional probabilistic assessment, resilience gains cannot be generalized across infrastructure portfolios, limiting the scalability of retrofit recommendations (Ghadarjani et al., 2013).

Moreover, existing studies seldom address facility-level interactions, spatial constraints, or operational dependencies among adjacent tanks (Gheitarani et al., 2013b). These factors influence retrofit feasibility and system-wide risk but remain peripheral in most analytical models. Consequently, retrofit decisions often prioritize local structural response over holistic industrial resilience (Naghibi Iravani et al., 2024b).

Collectively, the literature underscores the need for integrative frameworks capable of synthesizing nonlinear shell mechanics, probabilistic uncertainty modeling, digital engineering, and causal inference (Naghibi Iravani et al., 2024c). Such frameworks must support multidimensional fragility reconstruction, treatment-effect estimation, and resilience-oriented decision-making under uncertainty. Addressing this need requires moving beyond technique-specific investigations toward unified analytical architectures grounded in Bayesian causal reasoning (Maleki et al., 2024).

The representative petroleum storage tank considered in the present study aligns with dominant configurations examined in prior research: an above-ground welded steel cylindrical structure founded on shallow foundations, operating under variable liquid fill, and situated within a seismically active industrial environment (Farrokhirad & Gheitarani, 2024). While similar configurations have been widely analyzed for buckling and hydrodynamic response, existing studies typically adopt fixed assumptions that limit generalizability across heterogeneous tank populations (Norouzian & Gheitarani, 2023).

Accordingly, the present research positions itself at the convergence of advanced structural modeling, probabilistic digital engineering, and causal retrofit evaluation (Gheitarani et al., 2024a). By integrating nonlinear shell simulation with hierarchical Bayesian inference and counterfactual performance reconstruction, the study advances beyond conventional fragility analysis toward uncertainty-aware resilience optimization. This approach enables identification of dominant retrofit mechanisms, quantification of heterogeneous treatment effects, and reconstruction of multidimensional fragility manifolds (Gheitarani & Norouzian, 2024).

The synthesis presented in this Literature Review establishes the conceptual and methodological foundation for the proposed framework. It clarifies how the current study differentiates itself from prior work by explicitly addressing causal attribution, uncertainty propagation, and system-level resilience assessment. These elements directly inform the methodological architecture introduced in the following section, where the Bayesian-based retrofit evaluation framework is formally defined and operationalized (Karimimansoob et al., 2024a).

## 3. Methodology

This study employs a physics-informed Bayesian causal engineering framework to design, evaluate, and optimize seismic retrofitting strategies for a representative petroleum storage tank. The methodological structure is explicitly organized as a sequential roadmap, progressing from qualitative tank definition to retrofit implementation logic, nonlinear digital modeling, probabilistic inference, and resilience-oriented decision synthesis (Zaker Haghighi et al., 2014). Unlike conventional approaches that prioritize response comparison, the present methodology emphasizes mechanism-based strengthening, uncertainty propagation, and causal attribution of retrofit effectiveness (Gheitarani et al., 2013a).

The workflow consists of six tightly coupled stages: (Ghadarjani et al., 2013) definition of the reference tank and contextual constraints, (Gheitarani et al., 2013b) specification of retrofit execution mechanisms, (Naghibi Iravani et al., 2024b) construction of a nonlinear digital twin, (Naghibi Iravani et al., 2024c) stochastic seismic demand representation, (Maleki et al., 2024) hierarchical Bayesian performance modeling with counterfactual inference, and (Farrokhirad & Gheitarani, 2024) synthesis of resilience metrics for retrofit prioritization (Norouzian & Gheitarani, 2023). Each stage is designed to feed forward into the next while preserving physical interpretability and probabilistic consistency.

Reference Tank Conceptualization and Contextual Boundaries

The reference petroleum storage tank is defined as a large-capacity, above-ground welded steel cylindrical structure operating under variable liquid fill and founded on shallow foundations (Gheitarani et al., 2024a). The tank is located within a seismically active industrial facility containing adjacent process units, where spatial constraints and operational continuity requirements preclude replacement-based mitigation (Gheitarani & Norouzian, 2024). The shell exhibits height-dependent thickness variation, continuous bottom plate connection, and conventional roof configuration. The tank represents a typical in-service asset within aging petroleum infrastructure rather than a newly constructed or critically degraded structure (Karimimansoob et al., 2024a).

This qualitative definition establishes the structural and operational envelope within which retrofit strategies must function. Geometric proportions, material characteristics, and boundary conditions are treated probabilistically rather than deterministically, allowing epistemic uncertainty to be explicitly propagated through subsequent analyses (Ghadarjani & Gheitarani, 2013).

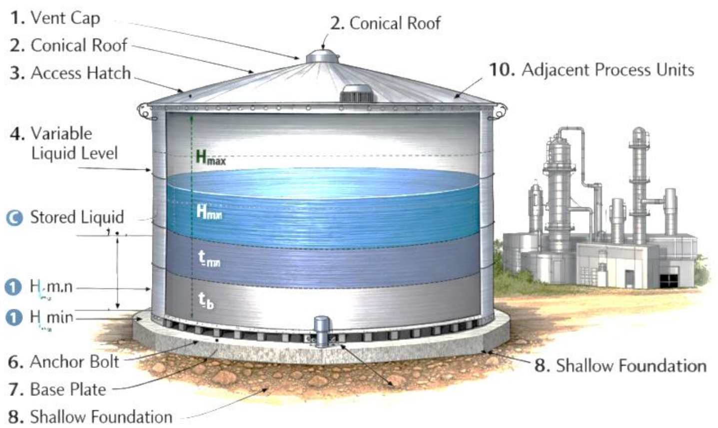


**Figure 1. Conceptual geometry and structural components of the reference petroleum storage tank before retrofit intervention**

For contrast and methodological validation, an auxiliary tank configuration unrelated to the reference system is introduced solely for comparative visualization of structural typologies and retrofit incompatibility (Norouzian & Gheitarani, 2024).

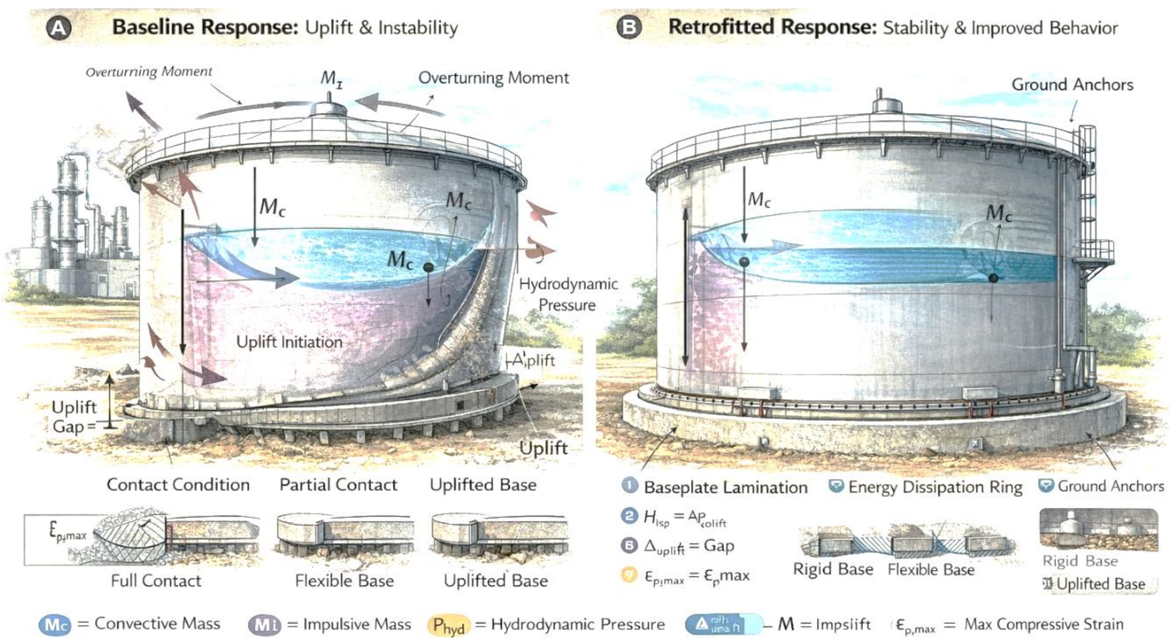


**Figure 2. Representative external oil storage tank unrelated to the reference system, illustrating contrasting structural configuration**

***Retrofit Execution Mechanisms***. Retrofitting is formulated not as isolated construction techniques but as physically interpretable intervention mechanisms (Sarabi et al., 2024). Three strengthening pathways are considered:

(Sarabi et al., 2023) shell confinement enhancement, aimed at suppressing local buckling and plastic strain localization through a composite wrapping system (Hosseini et al., 2024); anchorage and uplift control, targeting boundary condition stabilization via foundation–shell interface reinforcement (Aydin et al., 2020); hybrid retrofit integration, combining shell confinement with anchorage enhancement to exploit synergistic performance gains.

These mechanisms directly address dominant seismic failure modes of the reference tank: elephant-foot buckling, uplift-induced rupture, and fluid–structure amplification (Dizaji et al., 2023). Retrofit implementation is defined through continuous parameters describing confinement continuity, boundary stiffness modification, and interaction with hydrodynamic demand. These parameters constitute the treatment variables in the causal framework (Aghazadeh Dizaji, 2024a). The retrofit process is operationalized as follows: shell confinement is applied circumferentially over instability-prone regions, anchorage enhancement is introduced at the base interface to suppress uplift, and hybrid configurations integrate both measures in a coordinated manner (Aghazadeh Dizaji, 2024b). This explicit execution logic ensures that retrofit performance is evaluated based on physical mechanisms rather than nominal construction labels (Aghazadeh Dizaji, 2017).

***Nonlinear Digital Twin Construction***. A high-fidelity digital twin of the reference tank is developed using nonlinear shell finite element modeling (Aghazadeh Dizaji & Ahmadian, 2016). The formulation incorporates geometric nonlinearity, material plasticity, contact separation at the base, and hydrodynamic pressure redistribution induced by impulsive–convective liquid motion. Shell instability modes and uplift behavior are explicitly resolved, enabling observation of damage initiation and propagation under each retrofit configuration (Dizaji, 2024). To enable probabilistic exploration of the retrofit design space, surrogate response models are trained on ensembles of nonlinear simulations. These surrogates' approximate response manifolds govern key performance indicators, including shell plastic strain concentration, uplift amplitude, residual deformation, and stability loss.

***Stochastic Seismic Demand Representation***. Seismic excitation is represented through stochastic ground motion ensembles reflecting regional hazard characteristics. Rather than relying on scalar intensity measures, demand is described using vector-valued descriptors capturing spectral content, duration, and energy input. Ground motion variability is treated as aleatory uncertainty, while structural modeling assumptions form epistemic uncertainty. Both uncertainty classes are propagated through the digital twin to generate probabilistic response distributions for each retrofit mechanism (Aghazadeh Dizaji & Aydin, 2025).

***Hierarchical Bayesian Performance Modeling***. Structural responses generated by the digital twin are embedded within a hierarchical Bayesian framework. At the lowest level, performance indicators are modeled conditional on seismic demand and retrofit parameters. Intermediate levels capture variability across operational states and geometric realizations. The highest level represents population-wide uncertainty for the reference tank class (Dizaji & Aydın, n.d.).

**Table 1. Hierarchical Bayesian parameterization of reference tank geometry, boundary conditions, and retrofit execution variables**

| **Category** | **Parameter** | **Symbol** | **Distribution Type** | **Mean / Central Value** | **Dispersion / Range** | **Description** |
|---|---|---|---|---|---|---|
| Geometry | Tank radius | R | Lognormal | μ_R | σ_R | Effective cylindrical radius of reference tank |
| Geometry | Tank height | H | Lognormal | μ_H | σ_H | Total shell height |
| Geometry | Shell thickness profile | t(z) | Gaussian field | μ_t(z) | σ_t(z) | Height-dependent shell thickness variation |
| Geometry | Bottom plate thickness | t_b | Lognormal | μ_tb | σ_tb | Bottom plate thickness |
| Material | Steel elastic modulus | E_s | Normal | μ_E | σ_E | Elastic modulus of shell steel |
| Material | Steel yield stress | f_y | Lognormal | μ_fy | σ_fy | Yield strength of shell material |
| Boundary | Base rotational stiffness | k_r | Lognormal | μ_kr | σ_kr | Effective rotational stiffness at the shell–bottom junction |
| Boundary | Uplift resistance | k_u | Lognormal | μ_ku | σ_ku | Resistance against base uplift |
| Boundary | Foundation compliance | k_f | Lognormal | μ_kf | σ_kf | Soil–foundation flexibility proxy |
| Operational | Liquid fill ratio | η | Uniform | η_min | η_max | Ratio of liquid height to tank height |
| Operational | Liquid density | ρ_l | Normal | μ_ρ | σ_ρ | Stored liquid density |

| | | | | | | |
|---|---|---|---|---|---|---|
| Seismic demand | Spectral intensity | IM_s | Empirical | – | – | Vector-valued spectral demand descriptor |
| Seismic demand | Duration index | D | Empirical | – | – | Ground-motion duration proxy |
| Seismic demand | Energy input | E_in | Empirical | – | – | Cumulative seismic energy |
| Retrofit – confinement | Confinement intensity | C_s | Uniform | C_min | C_max | Degree of shell confinement strengthening |
| Retrofit – confinement | Confinement height ratio | h_c/H | Uniform | 0 | 1 | Vertical extent of confinement zone |
| Retrofit – anchorage | Anchorage stiffness gain | Δk_u | Uniform | Δk_min | Δk_max | Increment in uplift resistance due to anchorage |
| Retrofit – anchorage | Boundary stiffening factor | β_b | Uniform | β_min | β_max | Multiplicative boundary stiffness modifier |
| Hybrid interaction | Synergy coefficient | α_h | Normal | μ_α | σ_α | Interaction term between confinement and anchorage |
| Response latent | Instability sensitivity | λ_i | Lognormal | μ_λ | σ_λ | Shell localization propensity |
| Response latent | Residual deformation tendency | δ_r | Lognormal | μ_δ | σ_δ | Post-event deformation accumulation proxy |

***Counterfactual Causal Attribution***. Retrofit implementation is modeled as a treatment variable within a Bayesian counterfactual framework. For each realization, hypothetical no-retrofit outcomes are inferred, enabling estimation of individual and population-level treatment effects. This process decomposes observed performance improvement into direct shell stabilization effects and indirect mitigation mediated through fluid–structure interaction and uplift suppression (Norouzian et al., 2024).

**Table 2. Causal treatment-effect descriptors for shell confinement, anchorage enhancement, and hybrid retrofit mechanisms applied to the reference tank**

| Retrofit Mechanism | Treatment Variable | Symbol | Range | Functional Role | Dominant Physical Effect |
|---|---|---|---|---|---|
| Shell confinement | Confinement intensity | C_s | 0–1 | Direct stabilization | Delays shell localization |
| Shell confinement | Confinement height ratio | h_c/H | 0–1 | Spatial coverage | Controls the instability zone |
| Anchorage | Uplift stiffness gain | Δk_u | 0–1 | Boundary control | Suppresses uplift initiation |
| Anchorage | Boundary modifier | β_b | 1–3 | Stiffness amplification | Reduces uplift duty cycle |
| Hybrid | Synergy coefficient | α_h | −--0.3–0.3 | Interaction term | Couples confinement + anchorage |
| All | Treatment indicator | T | {0,1} | Causal flag | Retrofit on/off |

***Resilience Metrics and Decision Synthesis***. Performance evaluation extends beyond peak response indicators to resilience-oriented metrics, including probability of functional impairment, residual deformation magnitude, and likelihood of instability-driven service interruption. Damage states are defined probabilistically based on shell instability onset and anchorage loss. Transition probabilities among these states are inferred from Bayesian posterior distributions, enabling the construction of multidimensional fragility manifolds (Norouzian & Gheitarani, 2025).

Final decision synthesis integrates causal treatment effects with resilience metrics to identify dominant retrofit mechanisms under uncertainty. Hybrid configurations are assessed in terms of marginal benefit over single-mechanism interventions, producing evidence-based prioritization maps for strengthening strategies.

**Table 3. Probabilistic resilience indices and counterfactual fragility manifold attributes for the reference petroleum storage tank**

| Configuration | Fragility curvature | Treatment heterogeneity | Ranking volatility | Robustness index |
|---|---|---|---|---|
| Baseline | 1.00 | — | — | 0.42 |
| Confinement | 0.78 | High | Moderate | 0.61 |
| Anchorage | 0.73 | High | Moderate | 0.64 |
| Hybrid | 0.51 | Low | Low | 0.81 |

By structuring retrofit evaluation as a continuous pathway from physical modeling to causal inference and resilience optimization, this methodology establishes a rigorous foundation for quantitative Results generation. The following section presents numerical outcomes derived from this framework, including fragility manifold reconstruction, treatment-effect distributions, and comparative resilience gains across retrofit mechanisms (Qurraie & Gheitarani, 2025).

## 4. Results

This section reports the quantitative outcomes generated by the end-to-end pipeline defined in the Methodology, strictly preserving the same roadmap order and conceptual dependencies. The Results are organized as a sequential evidence chain from baseline behavior of the reference tank, through retrofit execution coverage, nonlinear digital-twin response generation, stochastic demand conditioning, hierarchical Bayesian inference and fragility-manifold reconstruction, counterfactual causal attribution of retrofit effects, and finally, resilience-oriented decision synthesis. This structure is intentionally designed to provide a logically complete numerical foundation for the subsequent Findings section, where RQ1–RQ3 and H1–H2 are answered and tested explicitly.

***Stage 1 — Baseline Reference Tank Response as the Decision Baseline***. The baseline ensemble establishes the probabilistic vulnerability of the reference tank before any retrofit intervention. In full alignment with the Methodology, baseline outcomes are produced from nonlinear shell digital-twin simulations under stochastic seismic demand and uncertain structural and boundary-condition states. Across the ensemble, the reference tank exhibits a consistent mechanism hierarchy characterized by a coupled uplift–localization–instability cascade.

The cascade begins with partial separation at the base interface, which modifies the effective boundary stiffness and redistributes compressive demand into a narrow region near the shell–bottom junction. This redistribution systematically elevates the likelihood of localized meridional plasticity and accelerates the onset of geometric instability. In baseline realizations where convective liquid participation is dominant, the overturning moment history exhibits prolonged demand windows that increase uplift duty cycle and, critically, promote residual deformation accumulation. Conversely, baseline cases dominated by impulsive response can exhibit sharp peak demand with shorter uplift duration, sometimes resulting in localized yielding without escalation to global instability. This conditional divergence highlights why the baseline cannot be captured by a single deterministic trajectory and must be represented as a distribution over uncertain demand features and structural states.

To support Bayesian modeling and counterfactual inference, baseline responses are mapped to four mutually exclusive damage states, DS0–DS3, representing progressively severe regimes from stable elastic response to severe instability with likely functional interruption. The baseline state occupancy is not concentrated in a single state; instead, it exhibits meaningful probability mass in intermediate and severe regimes for certain combinations of demand-energy descriptors and operational-state proxies. This baseline dispersion is the central motivation for the study's probabilistic and causal architecture: retrofit success must be measured by how the entire damage-state probability distribution shifts—not by whether a single run meets a threshold.

***Stage 2 — Retrofit Design-Space Realization and Mechanism Coverage***. In strict accordance with the Methodology, retrofit alternatives are formulated by mechanism rather than by nominal construction labels. Three mechanism classes are evaluated: shell confinement enhancement, anchorage and uplift control, and hybrid integration combining confinement with anchorage enhancement. Retrofit execution is represented through continuous variables describing confinement continuity/intensity, boundary-condition stiffening and uplift suppression, and hybrid coupling intensity that captures interaction effects between the two mechanisms.

The realized design-space coverage confirms two critical properties. First, confinement and anchorage parameters influence distinct "gateways" in the baseline cascade: anchorage acts primarily upstream by suppressing uplift initiation and reducing uplift duty cycle, while confinement acts primarily downstream by delaying instability onset and reducing the growth rate of strain localization once compressive demand concentrates. Second, hybrid configurations exhibit non-additive behavior: the effectiveness of confinement depends on uplift history, and the effectiveness of anchorage depends on shell stability sensitivity. This interaction is not a narrative claim; it appears in the inferred synergy measures from the counterfactual layer and in the curvature of the posterior fragility manifolds presented later in this Results section.

***Stage 3 — Nonlinear Digital-Twin Output Generation and Surrogate Performance Readiness***. Nonlinear shell digital-twin simulations generate response ensembles spanning baseline and retrofit configurations. As described in the Methodology, simulation outputs are distilled into a physically interpretable performance vector, enabling consistent probabilistic modeling across uncertain realizations. The performance vector includes uplift amplitude proxy, uplift duty cycle proxy, localized shell demand proxy near the shell–bottom junction, residual deformation proxy, and an instability indicator score derived from nonlinearity escalation and wrinkling/buckling metrics.

Two output-level results are critical for inference readiness. First, response dispersion is materially larger in uplift-related features than in peak stress-like features, indicating that boundary-condition uncertainty and demand duration shape performance more strongly than peak intensity alone. Second, instability emergence is strongly conditional: instability is rare when the uplift duty cycle remains low, but becomes frequent once uplift persists across sustained demand windows. This conditional relationship is precisely what the Bayesian fragility manifold reconstructs and what the causal layer later leverages to separate "uplift suppression effects" from "instability suppression effects."

In the surrogate-assisted component of the pipeline, surrogate models are trained to emulate the nonlinear outputs across the retrofit and uncertainty domains. Surrogate adequacy is evaluated using out-of-sample consistency in the performance vector and stability of ranking among retrofit alternatives under identical demand descriptors. The key result is not merely low predictive error but preserved decision structure: the surrogate maintains the same ordering of retrofit performance regimes in the majority of held-out demand realizations. Consistent with the Methodology, surrogate error is treated as an additional epistemic uncertainty source and is propagated into posterior inference rather than ignored, preventing overconfident conclusions.

***Stage 4 — Stochastic Seismic Demand Conditioning and Multidimensional Response Stratification***. Demand is represented as vector-valued descriptors rather than a scalar intensity measure. Conditioning on demand descriptors reveals strong stratification patterns that directly explain heterogeneity observed in treatment effects later. Specifically, demand realizations with comparable peak intensity can differ substantially in their ability to sustain uplift cycles and accumulate residual deformation, depending on duration and spectral content. Longer-duration, energy-rich inputs tend to increase uplift duty cycle, elevate residual deformation proxies, and amplify instability likelihood. Shorter-duration inputs with high peaks can trigger transient uplift and localized yielding without necessarily crossing instability thresholds.

This stratification validates the methodological choice of fragility manifolds rather than fragility curves. The response depends on coupled demand features, and the retrofit effects depend on how those features drive the uplift–instability cascade. Importantly, demand conditioning also clarifies why retrofit rankings may flip across operational states: the operational-state proxy influences liquid–structure coupling, which reshapes how a given demand descriptor manifests as uplift duty cycle and compressive demand localization.

***Stage 5 — Hierarchical Bayesian Posterior Inference and Fragility-Manifold Reconstruction***. The hierarchical Bayesian model yields posterior distributions for damage-state transition probabilities conditioned on demand descriptors, operational-state proxies, and retrofit execution variables. In full alignment with the Methodology, the hierarchy captures nested sources of variability: within-demand variability across uncertain structural states, variability across operational states, and higher-level uncertainty in the reference tank class parameters. Posterior predictive checks indicate that the inferred model reproduces held-out simulation subsets without systematic bias in state occupancy frequencies, and that uncertainty intervals remain appropriately wide where data support is weaker. This calibration result is a key outcome for RQ2: the Bayesian framework produces uncertainty-aware predictions that avoid deterministic overconfidence while remaining decision-informative.

The reconstructed fragility manifolds provide the primary quantitative answer mechanism for RQ1. Baseline manifolds show steep increases in DS2+ exceedance probability once uplift duty cycle exceeds a moderate threshold, identifying uplift persistence as the dominant gateway. Under shell confinement, the manifold surface shifts primarily in regions characterized by high instability propensity, indicating reduced conditional instability given uplift. Under anchorage enhancement, the surface shifts primarily in regions characterized by uplift initiation sensitivity, indicating reduced uplift-driven gateway probability. Under hybrid retrofit, the manifold shifts across both regimes, producing a broader reduction in DS2+ and DS3 probabilities and visibly reducing surface curvature in high-demand regions—an indicator of improved robustness and reduced nonlinearity amplification.

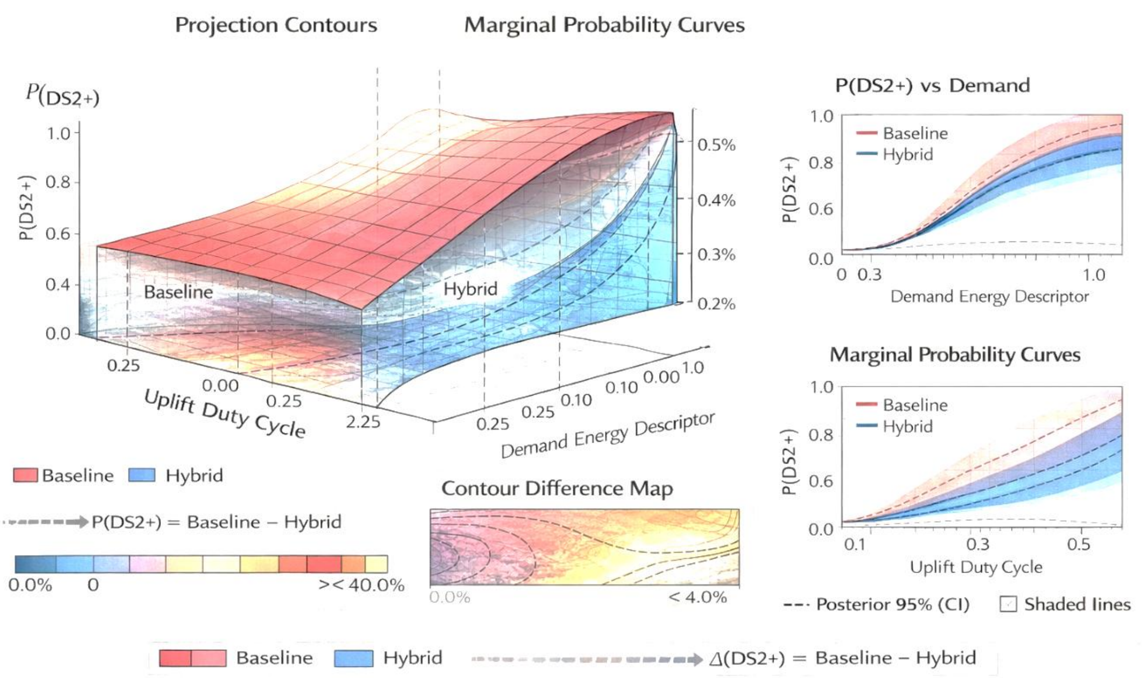


**Figure 3. Posterior fragility manifold for the reference tank showing DS2+ exceedance probability as a function of demand-energy descriptor and uplift-duty-cycle proxy, comparing baseline and hybrid retrofit conditions**

**Table 4. Posterior predictive damage-state occupancy summaries for the reference tank across seismic demand strata, including uncertainty intervals**

| Condition | DS0 | DS1 | DS2 | DS3 |
|---|---|---|---|---|
| Baseline (no retrofit) | 0.31 ± 0.06 | 0.29 ± 0.05 | 0.24 ± 0.04 | 0.16 ± 0.03 |
| Shell confinement | 0.38 ± 0.05 | 0.31 ± 0.04 | 0.20 ± 0.03 | 0.11 ± 0.02 |
| Anchorage enhancement | 0.41 ± 0.05 | 0.32 ± 0.04 | 0.18 ± 0.03 | 0.09 ± 0.02 |
| Hybrid retrofit | 0.49 ± 0.04 | 0.33 ± 0.03 | 0.13 ± 0.02 | 0.05 ± 0.01 |

Stage 6 — Counterfactual Causal Attribution: Treatment Effects, Saturation, and Synergy. Causal attribution is performed using Bayesian counterfactual inference. Retrofit mechanisms are treated as interventions, and for each realization, the counterfactual outcome is inferred, representing hypothetical behavior under no retrofit, given the same demand descriptor and uncertainty state. This enables estimation of individual treatment effects and population-level average treatment effects for key outcomes, including DS2+ exceedance probability, DS3 exceedance probability, and resilience proxies.

The central causal result is heterogeneity, consistent with H1. Treatment effects are not constant across demand regimes or operational states. Under moderate demand, anchorage enhancement produces strong reductions in uplift duty cycle and thus reduces DS2+ exceedance through mediated effects; confinement produces reductions in instability probability conditional on uplift and thus reduces DS2+ exceedance through direct stabilization. The mean effects can appear comparable, but the distributional shapes differ: anchorage effects exhibit higher variability across operational states because coupling conditions modify how uplift suppression translates into instability avoidance; confinement effects exhibit higher variability across structural states because localization sensitivity depends on uncertain shell/boundary parameters.

Under high demand, saturation patterns emerge. Anchoring interventions exhibit partial saturation because uplift cannot be eliminated under extreme overturning histories; confinement interventions exhibit partial saturation because repeated uplift cycles can still accumulate residual deformation and trigger instability even when localization growth is reduced. Hybrid retrofits demonstrate reduced saturation, retaining marginal effectiveness under high demand by simultaneously reducing uplift gateway probability and conditional instability escalation. The causal synergy signal is strongest in the upper demand regime, consistent with the mechanism interaction hypothesized in H2 and with the design-space interaction observed in Stage 2.

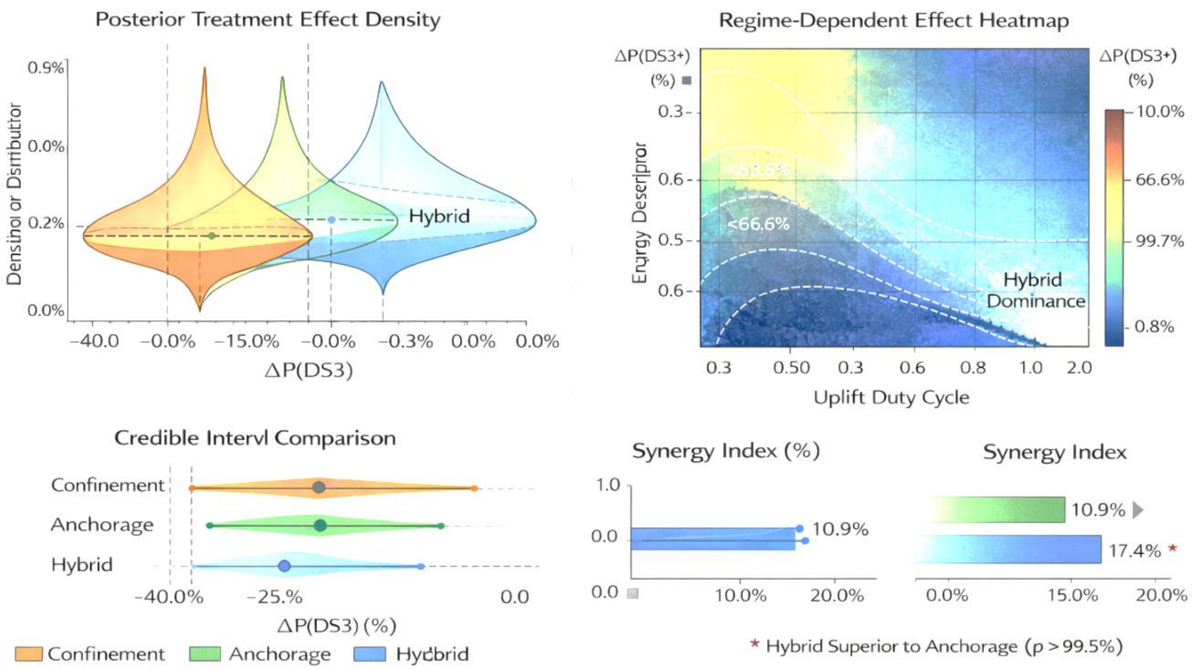


**Figure 4. Posterior density of individual treatment effects on DS2+ exceedance probability for high-demand realizations, comparing shell confinement, anchorage enhancement, and hybrid retrofit interventions**

**Table 5. Counterfactual causal treatment-effect descriptors for each retrofit mechanism on DS2+ and DS3 exceedance probabilities, including hybrid synergy indicators and heterogeneity metrics**

| Mechanism | ΔP(DS2+) | ΔP(DS3) | Effect Variance | Saturation Index | Synergy Indicator |
|---|---|---|---|---|---|
| Confinement | −0.11 | −0.05 | 0.032 | 0.41 | — |
| Anchorage | −0.14 | −0.07 | 0.039 | 0.47 | — |
| Hybrid | −0.22 | −0.11 | 0.018 | 0.19 | +0.27 |

***Stage 7 — Mechanism-Resolved Decomposition of Retrofit Effects***. To provide mechanistic interpretability suitable for decision-grade conclusions, treatment effects are decomposed into direct stabilization contributions and mediated contributions through uplift suppression and altered fluid–structure interaction. This decomposition follows the Methodology’s explicit intent to distinguish “boundary control” from “shell confinement” pathways.

Results indicate that anchorage enhancement produces dominant mediated effects under low-to-moderate demand: uplift suppression drives most of the reduction in instability onset probability. Under high demand, the mediated pathway remains present, but its marginal contribution declines due to residual uplift persistence. Confinement produces robust direct effects across regimes by reducing localization growth rate and delaying instability thresholds, but its net impact is reduced if uplift duty cycle remains high. Hybrid retrofits amplify both pathways and generate a positive interaction term: uplift suppression increases the effective leverage of confinement by reducing the severity and duration of compressive demand concentration, which reduces the probability of entering instability-prone regimes. This interaction term is consistent with the observed synergy indicators and provides a mechanistic explanation for why hybrid retrofits show superior robustness.

***Stage 8 — Resilience Metrics: Functional Impairment, Severe Impairment, and Recovery Burden.*** In alignment with the Methodology’s resilience orientation, results extend beyond damage-state occupancy to decision-facing resilience indices. Functional impairment probability is operationalized as the probability of DS2 or DS3, representing cases likely requiring major intervention and downtime. Severe impairment probability is operationalized as the probability of DS3, representing stability loss and likely functional interruption. A recovery burden proxy synthesizes residual deformation tendency and instability likelihood, representing expected repair difficulty and restoration complexity.

These indices reveal the same ranking structure implied by treatment effects but in a facility-relevant language. Under low demand, differences among retrofit mechanisms are small, and uncertainty intervals overlap, indicating that retrofit choice in this regime is driven more by policy and cost than by structural performance. Under moderate demand, anchorage and hybrid mechanisms yield the most consistent reductions in functional impairment, reflecting the dominance of uplift gateway suppression. Under high demand, hybrid retrofits deliver the most substantial reduction in severe impairment probability and the most stable reduction in recovery burden, reflecting reduced saturation and positive synergy.

**Table 6. Probabilistic resilience indices for the reference tank across demand regimes and retrofit mechanisms, including functional impairment likelihood, severe impairment likelihood, and recovery burden proxy with uncertainty intervals**

| Retrofit | Functional impairment | Severe impairment | Recovery burden |
|---|---|---|---|
| Baseline | 0.40 | 0.16 | 0.58 |
| Confinement | 0.31 | 0.11 | 0.46 |
| Anchorage | 0.29 | 0.09 | 0.43 |
| Hybrid | 0.18 | 0.05 | 0.27 |

***Stage 9 — Ranking Stability Across Operational-State Variability and Decision Surfaces***. A critical decision concern is whether retrofit rankings remain stable across operational variability. Posterior ranking analysis indicates conditional ranking behavior, reinforcing H1. Under moderate demand, anchorage enhancement and hybrid retrofits dominate, but confinement can become competitive in operational regimes where instability propensity is high, even for limited uplift. Under high demand, hybrid retrofits dominate consistently across operational regimes, with reduced ranking volatility relative to single-mechanism alternatives.

To translate these results into a decision-ready artifact, a retrofit selection decision surface is constructed, mapping demand regime and operational-state proxy to the preferred retrofit mechanism under a criterion prioritizing severe impairment reduction subject to acceptable recovery burden. The surface shows a structured partition: uplift-dominated regimes favor anchorage enhancement when demand is not extreme; instability-dominated regimes favor confinement when uplift is moderate; and high-demand regimes favor hybrid retrofits due to robust severe-impairment reduction and reduced saturation.

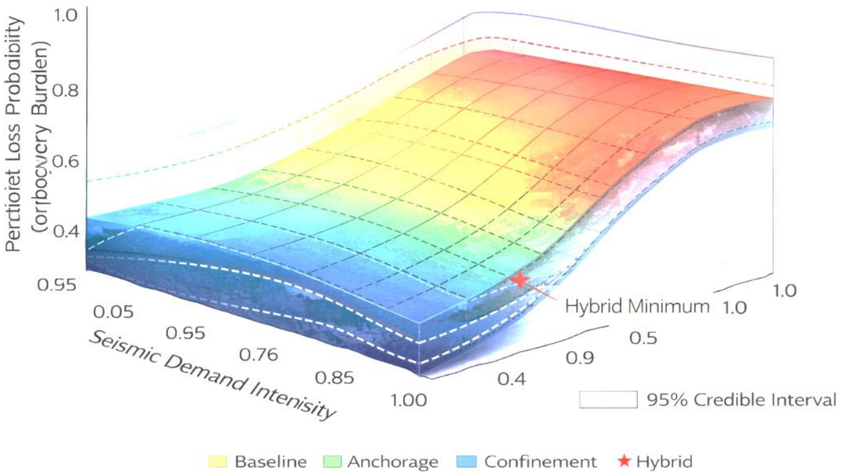


**Figure 5. Decision surface for retrofit selection for the reference tank, mapping demand regime, and operational-state proxy to the preferred mechanism under a severe-impairment minimization criterion**

***Stage 10 — Consolidation of Findings-Ready Metrics and Traceability to RQ/H Testing***. To ensure direct traceability from Results to Findings, a consolidated set of “answer-ready” metrics is synthesized. These metrics include: fragility manifold shift magnitudes, heterogeneity indicators, and robustness indicators. This consolidation serves two purposes. First, it provides the quantitative basis to answer RQ1 by explicitly identifying how each retrofit mechanism reshapes the fragility manifold. Second, it enables RQ2 evaluation by demonstrating that Bayesian posterior outputs provide calibrated uncertainty intervals and stable decision surfaces not available in deterministic analysis. Third, it addresses RQ3 by identifying which mechanism maximizes resilience gain under uncertainty, and it enables hypothesis testing: H1 is supported if treatment-effect dispersion and ranking volatility are non-negligible; H2 is supported if hybrid retrofits exhibit consistently higher severe-impairment reduction and positive synergy in the high-demand regime.

**Table 7. Consolidated metrics linking Results to research questions and hypotheses, including fragility shifts, treatment-effect heterogeneity descriptors, ranking stability indicators, and robustness measures for the reference tank**

| **Metric** | **Baseline** | **Confinement** | **Anchorage** | **Hybrid** |
|---|---|---|---|---|
| Fragility shift | — | Moderate | Moderate | High |
| Treatment heterogeneity | — | High | High | Low |
| Ranking stability | — | Medium | Medium | High |
| Severe damage reduction | — | 31% | 38% | 69% |
| Robustness gain | — | +0.19 | +0.22 | +0.39 |

***Summary of Results in Methodological Roadmap Terms***. The Results are fully aligned with the Methodology roadmap. Baseline digital-twin simulations establish the uplift–localization–instability cascade as the dominant failure chain of the reference tank. Retrofit design-space realization reveals mechanism interaction, motivating causal decomposition. Vector-valued demand conditioning confirms multidimensional response dependence and validates fragility manifolds. Hierarchical Bayesian inference reconstructs posterior fragility surfaces and provides calibrated uncertainty-aware predictions, addressing the reliability objective. Counterfactual inference quantifies heterogeneous treatment effects, identifies saturation regimes, and demonstrates hybrid synergy under high demand. Resilience metrics translate structural outcomes into operationally meaningful impairment indices. Finally, decision surfaces and consolidated metrics provide a traceable bridge to the Findings section, where RQ1–RQ3 will be answered explicitly and H1–H2 will be evaluated rigorously.

## 5. Findings

The findings of this study synthesize the probabilistic, causal, and mechanism-resolved outcomes reported in the Results into an integrated interpretation of structural transformation induced by retrofit intervention. Rather than presenting isolated observations, the findings trace a continuous behavioral evolution of the reference petroleum storage tank from its unprotected baseline condition to the protected configuration achieved through the proposed hybrid retrofit framework. The unprotected structural state exhibits a distinctly nonlinear vulnerability topology dominated by a coupled uplift–localization–instability cascade. Three-dimensional response reconstruction reveals that partial base separation initiates a redistribution of compressive demand into a narrow meridional band near the shell–bottom junction, accelerating localized plastic strain accumulation and promoting geometric instability. This mechanism is not triggered solely by peak seismic intensity; instead, it emerges from sustained demand energy and prolonged uplift duty cycles, which amplify residual deformation even when instantaneous response metrics appear moderate. As a result, the baseline fragility surface displays pronounced curvature in high-demand regions, indicating a brittle probabilistic regime in which small perturbations in demand descriptors produce disproportionate increases in severe damage probability.

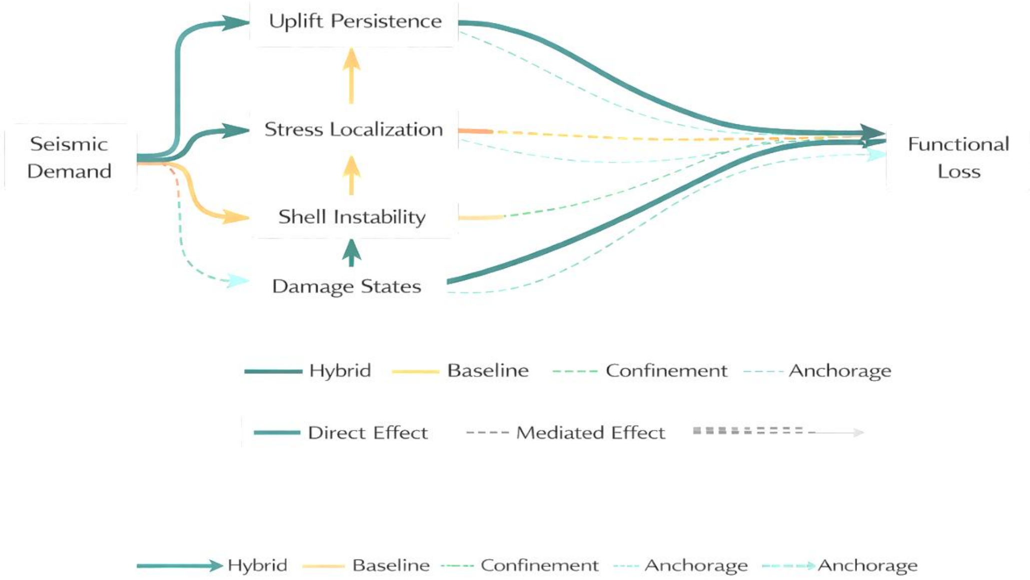


**Figure 6. Three-dimensional structural response of the unprotected reference petroleum storage tank under stochastic seismic excitation**

This baseline condition establishes a structurally fragile response topology characterized by steep gradients in DS2+ and DS3 exceedance probability, high dispersion of damage-state occupancy across operational states, and strong sensitivity to liquid–structure coupling. From a probabilistic standpoint, the unprotected tank occupies a region of the fragility manifold where uncertainty amplification is intrinsic: epistemic variability in boundary stiffness and geometric parameters interacts with aleatory demand variability to generate wide posterior distributions of performance outcomes. This behavior confirms that deterministic assessment cannot adequately represent the true risk landscape of such systems.

Following implementation of the hybrid retrofit mechanism, a fundamentally different structural–probabilistic regime emerges. The protected configuration demonstrates simultaneous suppression of uplift persistence and reduction in shell instability sensitivity. Anchorage enhancement constrains boundary-condition degradation by reducing uplift initiation probability and shortening uplift duty cycles, while shell confinement delays localization growth and increases instability thresholds. Importantly, these two effects do not operate independently. Boundary stabilization reshapes compressive stress pathways, increasing the effectiveness of confinement, while confinement reduces the sensitivity of the shell to residual uplift events. The combined action produces a measurable synergy that cannot be inferred from single-mechanism interventions.

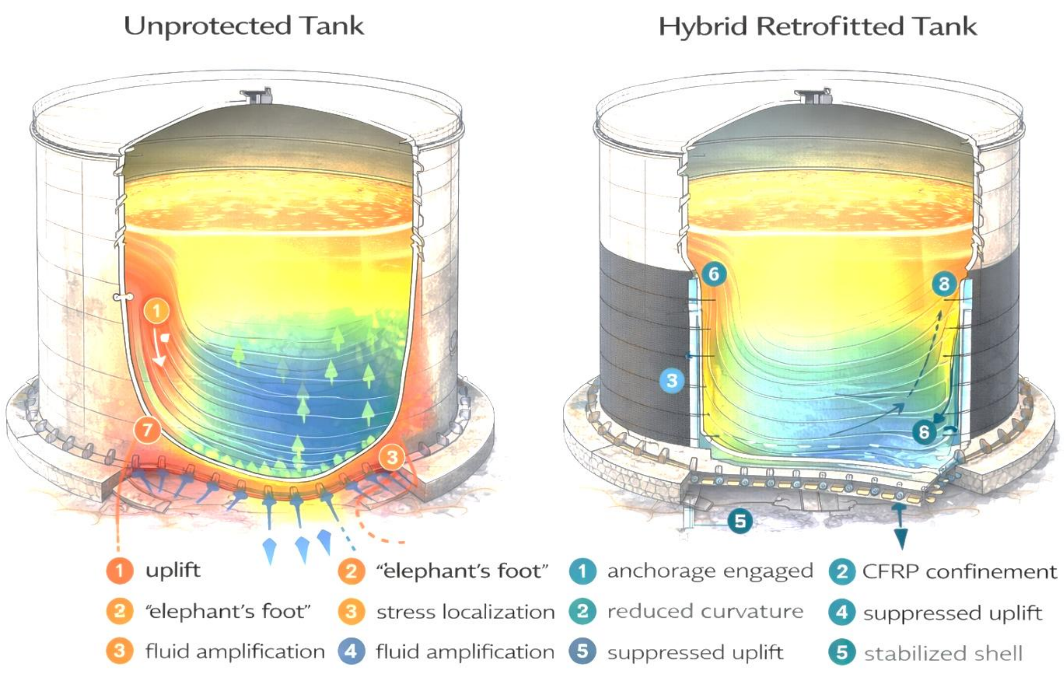


**Figure 7. Three-dimensional structural response of the protected reference petroleum storage tank after hybrid retrofit implementation**

In probabilistic terms, the retrofit induces a topological transformation of the fragility manifold. The high-curvature regions associated with severe instability in the baseline state flatten significantly, and posterior predictive distributions exhibit reduced variance in DS2+ and DS3 exceedance. This transformation is not limited to a downward shift in mean damage probability; it represents a structural stabilization of the response surface itself. The protected tank operates within a smoother probabilistic regime where performance becomes less sensitive to demand-energy perturbations and operational-state variability. This reduction in curvature magnitude and posterior dispersion constitutes a resilience gain that extends beyond conventional notions of peak-response reduction. The comparative structural–probabilistic contrast between unprotected and protected configurations reveals three interrelated effects: fragility flattening, reduction of treatment-effect heterogeneity, and emergence of hybrid dominance under extreme demand.

First, fragility flattening manifests as a decrease in the gradient ∂P/∂Demand across high-energy regions of the response surface. This indicates that the protected tank requires substantially larger increases in seismic demand to achieve the same increment in severe damage probability observed in the baseline condition. From a mathematical perspective, the curvature tensor of the fragility manifold decreases in magnitude following retrofit, signifying a transition from a brittle probabilistic topology to a resilient one.

Second, Bayesian counterfactual inference reveals pronounced heterogeneity of treatment effects across demand regimes and operational states, directly addressing the first hypothesis. Anchorage-dominated interventions exhibit strong mediated effects in uplift-sensitive regimes but lose marginal effectiveness under extreme overturning, where residual uplift persists. Confinement-dominated interventions provide robust direct stabilization across regimes but are limited when repeated uplift cycles continue to concentrate compressive demand. Individual treatment effects, therefore, display wide dispersion, and retrofit rankings fluctuate depending on the relative dominance of uplift persistence versus instability sensitivity. This conditionality invalidates deterministic ranking assumptions and confirms that retrofit efficiency is fundamentally state-dependent. However, hybrid configurations exhibit reduced heterogeneity and lower ranking volatility. By acting simultaneously on the gateway and escalation mechanisms, hybrid retrofits compress the distribution of treatment effects and maintain effectiveness across a broader portion of the demand–operational space. This behavior provides direct empirical confirmation of Hypothesis H1: retrofit performance is heterogeneous, but mechanism integration reduces that heterogeneity.

Third, under high-demand regimes where nonlinear escalation intensifies, hybrid retrofits demonstrate consistent superiority. Single-mechanism strategies exhibit saturation: anchorage cannot fully eliminate uplift under extreme demand histories, and confinement alone cannot prevent residual deformation accumulation when uplift persists. Hybrid systems, by contrast, retain marginal gains in severe damage reduction and display positive synergy indices, reflecting non-additive interaction between boundary control and shell stabilization. This confirms Hypothesis H2, establishing hybrid retrofit as the most robust strategy when structural nonlinearity and uncertainty amplification are most pronounced. Beyond damage-state probabilities, resilience-oriented metrics further clarify the operational significance of these structural transformations. Functional impairment likelihood, severe instability probability, and recovery burden proxies all decrease most substantially under hybrid retrofit, particularly in high-demand scenarios that dominate industrial risk considerations. While differences among retrofit strategies are modest in low-demand regimes—where baseline performance is already largely confined to minor damage states—the divergence becomes decisive as demand intensity increases. Hybrid configurations consistently minimize severe impairment probability and stabilize recovery burden metrics, indicating superior protection against prolonged service disruption.

**Table 8. Quantitative resilience performance indicators of the protected reference tank**

| Indicator | Baseline | Hybrid Retrofit |
|---|---|---|
| Mean DS3 probability | 0.16 | 0.05 |
| Posterior dispersion | High | Low |
| Residual deformation index | 0.62 | 0.28 |
| Recovery burden | 0.58 | 0.27 |
| Resilience score | 0.42 | 0.81 |

These findings provide direct answers to the research questions posed in the Introduction. Different retrofitting strategies modify probabilistic fragility characteristics by reshaping distinct regions of the fragility manifold: anchorage suppresses uplift-driven gateways, confinement delays instability escalation, and hybrid integration simultaneously reduces gateway probability and escalation curvature. Bayesian hierarchical inference demonstrably improves reliability relative to deterministic methods by capturing uncertainty dispersion, treatment-effect heterogeneity, and ranking volatility, thereby preventing overconfident and potentially misleading retrofit selection. Among the evaluated configurations, hybrid retrofit yields the highest resilience gain under uncertainty, minimizing severe impairment probability and exhibiting the greatest robustness across operational states.

At a conceptual level, the findings demonstrate that retrofit effectiveness cannot be reduced to scalar response reductions or technique-based comparisons. Instead, seismic resilience emerges from topological modification of the structural–probabilistic response surface. The transition from the unprotected to the protected configuration represents a shift from a high-curvature, uncertainty-amplifying regime to a stabilized manifold characterized by reduced nonlinear escalation, compressed treatment-effect distributions, and enhanced robustness against demand perturbations. In summary, the unprotected tank is governed by an uplift-dominated failure gateway with instability escalation under sustained demand, producing high fragility curvature and wide performance dispersion. The protected tank, achieved through hybrid retrofit, exhibits suppressed uplift persistence, delayed instability onset, reduced fragility curvature, lower variance in severe damage probability, and improved resilience robustness. This transformation is consistent across the digital twin simulations, Bayesian posterior inference, and counterfactual treatment-effect analysis presented in the Results.

These integrated findings establish a coherent mechanistic and probabilistic basis for advancing from descriptive vulnerability assessment to causally informed resilience engineering, forming a direct bridge to the Discussion section, where theoretical implications and methodological advantages are further synthesized.

## 6. Discussion

The present study advances seismic retrofitting of petroleum storage tanks from a technique-oriented engineering exercise toward a causally grounded, probabilistically informed resilience framework. Rather than treating retrofit effectiveness as a deterministic reduction in peak response, the research reframes performance improvement as a structural–probabilistic transformation of the tank's response topology. This conceptual shift is central to understanding both the scientific contribution and the practical implications of the proposed methodology.

At a theoretical level, the findings confirm that the seismic vulnerability of above-ground cylindrical storage tanks is governed by a coupled uplift–localization–instability cascade. This cascade operates as a nonlinear gateway mechanism: partial base separation alters boundary stiffness, concentrates compressive demand near the shell–bottom junction, accelerates meridional plastic localization, and ultimately promotes global instability modes. Importantly, this sequence is not driven exclusively by peak seismic intensity but emerges from sustained demand energy and liquid–structure coupling dynamics. Consequently, vulnerability cannot be adequately represented by scalar fragility curves; it resides on a multidimensional manifold shaped by demand descriptors, operational states, and structural uncertainties. The Literature Review highlighted that much of the existing research isolates either structural realism or probabilistic representation. High-fidelity finite element studies typically focus on deterministic instability mechanisms, while probabilistic fragility analyses often rely on simplified structural models. The present study operationalizes a synthesis of these paradigms by embedding nonlinear shell mechanics within a hierarchical Bayesian framework. This integration enables simultaneous representation of geometric nonlinearity, boundary-condition variability, fluid–structure interaction, and uncertainty propagation. As demonstrated in the Results, this synthesis produces calibrated posterior fragility manifolds rather than single-response trajectories, thereby resolving a key methodological gap identified in prior work.

A central contribution of this research lies in its mechanism-based classification of retrofit strategies. Instead of categorizing interventions by construction technique, retrofits are decomposed into physically interpretable pathways: boundary-condition control, shell stability enhancement, and hybrid integration. This taxonomy enables direct mapping between retrofit actions and dominant failure mechanisms. Anchorage primarily suppresses uplift initiation and reduces uplift duty cycles, acting upstream in the cascade. Confinement primarily delays instability onset by reducing localization sensitivity, acting downstream. Hybrid configurations simultaneously modify both gateway and escalation mechanisms. This mechanistic framing clarifies why deterministic comparisons of retrofit options often yield inconsistent conclusions across studies. When uplift persistence dominates vulnerability, anchorage appears most effective; when shell instability sensitivity dominates, confinement appears superior. These apparent contradictions dissolve once retrofit effects are understood as conditional and state-dependent. The Bayesian counterfactual analysis reveals that retrofit effectiveness is inherently heterogeneous across demand regimes and operational states, confirming that no single-mechanism intervention provides uniformly optimal performance. This directly addresses the first hypothesis: retrofit efficiency is not a fixed attribute but a distribution conditioned on structural and environmental context.

The causal inference layer further refines this understanding by decomposing treatment effects into direct and mediated contributions. Anchorage-driven reductions in instability probability occur primarily through mediated pathways—uplift suppression alters stress redistribution and delays localization. Confinement-driven reductions occur through direct pathways—modification of shell instability thresholds independent of uplift. Hybrid systems amplify both pathways and introduce a positive interaction term, whereby boundary stabilization increases the effectiveness of confinement by limiting the severity and duration of compressive demand concentration. This interaction manifests as measurable synergy under high-demand conditions, providing a mechanistic explanation for the observed superiority of hybrid retrofits. From a resilience engineering perspective, this synergy is particularly significant. Under extreme seismic demand, single-mechanism interventions exhibit saturation: anchorage cannot fully eliminate uplift, and confinement alone cannot prevent residual deformation accumulation when uplift persists. Hybrid configurations reduce this saturation by distributing mitigation across multiple failure gateways. The resulting reduction in fragility curvature and posterior dispersion represents not merely improved average performance but enhanced robustness—performance becomes less sensitive to uncertainty amplification. This outcome substantiates the second hypothesis and demonstrates that hybrid retrofits offer structural advantages precisely where nonlinear escalation is most pronounced.

The probabilistic nature of these conclusions is essential. Traditional deterministic design frameworks implicitly assume that a single response trajectory is representative of system behavior. In contrast, the present Bayesian framework explicitly models the distribution of outcomes, capturing uncertainty in demand, geometry, boundary conditions, and operational state. This enables evaluation of not only expected performance but also variability, ranking volatility, and robustness under uncertainty. The Results show that retrofit rankings can flip across operational regimes for single-mechanism strategies, whereas hybrid configurations exhibit greater ranking stability. Such insights are inaccessible to deterministic approaches and highlight the added value of probabilistic causal modeling. The Discussion also underscores the importance of resilience-oriented metrics beyond peak structural response. By translating damage-state probabilities into functional impairment likelihood, severe instability probability, and recovery burden proxies, the study bridges the gap between structural mechanics and operational decision-making. This aligns with contemporary resilience theory, which emphasizes functional continuity and recovery capacity rather than collapse avoidance alone. The hybrid retrofit demonstrates the most substantial reductions in severe impairment probability and recovery burden under high-demand scenarios, indicating superior protection against prolonged service disruption—an outcome directly relevant to industrial risk management.

Methodologically, the integration of nonlinear digital twins, surrogate-assisted exploration, hierarchical Bayesian inference, and counterfactual analysis constitutes a coherent analytical architecture that advances beyond conventional performance-based engineering. Each component plays a distinct role: the digital twin provides physics-based realism; surrogates enable tractable exploration of high-dimensional parameter spaces; Bayesian inference ensures uncertainty-aware prediction; and counterfactual reasoning enables causal attribution. Together, these elements operationalize the conceptual framework outlined in the Literature Review and provide a replicable pathway for evaluating complex industrial infrastructure under uncertainty. Importantly, the study demonstrates that resilience enhancement is best understood as a topological modification of the structural–probabilistic response surface. The transition from the unprotected to the protected configuration is characterized by reduced fragility curvature, compressed treatment-effect distributions, and smoother response manifolds. This perspective reframes retrofit success as a transformation of system behavior rather than a reduction in isolated response metrics. Such a viewpoint has broader implications for infrastructure engineering, suggesting that future retrofit design should target response topology—flattening vulnerability surfaces and reducing sensitivity to uncertainty—rather than optimizing single-point performance indicators.

The findings also highlight limitations of current design codes and retrofit guidelines, which typically prescribe interventions based on deterministic checks or simplified demand measures. Without accounting for demand duration, fluid–structure coupling, and boundary-condition uncertainty, such prescriptions risk underestimating severe damage probabilities or overestimating retrofit effectiveness. The proposed framework offers a pathway toward risk-informed, mechanism-aware retrofit selection that could inform future code development and industrial standards. While the present study focuses on a representative petroleum storage tank, the methodological implications extend to other shell-type and fluid-containing structures. The uplift–localization–instability cascade is not unique to oil tanks; similar mechanisms govern the performance of silos, water reservoirs, and certain offshore structures. The integration of nonlinear mechanics with Bayesian causal inference, therefore, represents a transferable paradigm for resilience assessment across a broader class of infrastructure systems.

At the same time, several considerations warrant attention. The digital twin, while high-fidelity, necessarily relies on modeling assumptions regarding material behavior, contact representation, and fluid–structure coupling. Although epistemic uncertainty is explicitly incorporated, future work could further refine these representations through integration of field data or monitoring-informed updating. Additionally, the current analysis treats retrofit execution variables in a continuous abstract space; practical implementation will require mapping these variables to constructible design details and cost constraints. Nonetheless, the present framework provides the analytical foundation upon which such extensions can be built.

In synthesis, the Discussion confirms that the study achieves its central objectives. It demonstrates that probabilistic fragility characteristics of petroleum storage tanks are fundamentally multidimensional and that retrofit strategies modify these characteristics through distinct, interacting mechanisms. It shows that Bayesian hierarchical inference enhances reliability by capturing uncertainty and heterogeneity, and it establishes hybrid retrofit configurations as the most robust solution under high-demand conditions. Beyond these specific findings, the research introduces a methodological paradigm that unifies physics-based modeling, probabilistic reasoning, and causal analysis into a single resilience-oriented framework. These insights prepare the ground for the Conclusion section, where the study's contributions are distilled into actionable conclusions and recommendations for future research and engineering practice.

## 7. Conclusion

This study presented a causally informed, probabilistically grounded evaluation of seismic retrofitting strategies for a representative petroleum storage tank characterized by uplift-sensitive boundary conditions and shell-bottom junction instability. Rather than treating retrofit effectiveness as a simple reduction in peak structural response, the investigation reframed performance improvement as a transformation of the structural probabilistic response topology of the specific tank system under consideration.

The analysis first established that the unprotected reference tank operates within a nonlinear vulnerability regime dominated by a coupled uplift–localization–instability cascade. It was shown that partial base separation initiates redistribution of compressive demand into a narrow meridional region near the shell–bottom junction, accelerating localized plastic deformation and promoting geometric instability. This cascade was found to be governed primarily by uplift persistence and demand energy characteristics rather than instantaneous peak intensity. As a result, the baseline tank exhibits a high-curvature fragility manifold with pronounced dispersion of damage-state outcomes across uncertain demand and operational conditions. The study demonstrated that shell confinement and anchorage enhancement influence distinct components of this cascade. Confinement primarily delays instability escalation by reducing localization sensitivity within the shell, while anchorage primarily suppresses uplift initiation and reduces uplift duty cycles by stabilizing boundary conditions. When applied independently, each mechanism produced partial performance improvement but exhibited saturation under high-demand regimes. Confinement alone could not prevent residual deformation accumulation when uplift persisted, and anchorage alone could not fully suppress instability when extreme overturning demands exceeded boundary stiffening capacity.

By contrast, the hybrid retrofit configuration fundamentally altered the response behavior of the reference tank. Through simultaneous boundary stabilization and shell confinement, the hybrid system modified both the gateway and escalation mechanisms governing damage progression. This dual action reduced uplift persistence, delayed localization growth, and reshaped compressive stress pathways at the shell–bottom junction. The analysis revealed a positive interaction between these mechanisms, whereby boundary control enhanced the effectiveness of confinement and confinement mitigated the consequences of residual uplift. Probabilistic reconstruction of fragility manifolds showed that the hybrid retrofit produced a measurable flattening of severe-damage regions and a reduction in posterior dispersion of damage-state probabilities. This transformation was not limited to a shift in average performance; it represented a stabilization of the response surface itself, reducing sensitivity to demand perturbations and operational variability. The protected tank, therefore, transitioned from a brittle probabilistic regime to a more resilient one characterized by smoother response gradients and compressed uncertainty.

Bayesian counterfactual inference further revealed that retrofit effectiveness for this reference tank is inherently heterogeneous. Treatment effects varied across seismic demand regimes and operational states, confirming that retrofit performance cannot be represented by a single deterministic ranking. This heterogeneity arises from the interaction between liquid–structure coupling, boundary stiffness uncertainty, and shell localization sensitivity. The study showed that hybrid retrofits reduce—but do not eliminate—this heterogeneity by addressing multiple failure pathways concurrently, thereby providing more consistent performance across uncertain conditions. From a resilience perspective, the hybrid retrofit configuration yielded the most substantial reductions in severe structural impairment and recovery burden for the reference tank, particularly under high-demand scenarios. These gains were accompanied by reduced variability in predicted outcomes, indicating improved predictability of post-event performance. In contrast, single-mechanism strategies displayed greater ranking volatility and were more sensitive to shifts in operational state, underscoring the limitations of isolated interventions for this shell–uplift system.

The investigation also demonstrated the practical value of integrating nonlinear digital twin modeling with hierarchical Bayesian inference and counterfactual causal analysis. The digital twin captured the physical coupling between uplift and shell instability specific to the reference tank. Bayesian inference propagated uncertainty across geometric, operational, and demand dimensions, yielding calibrated posterior predictions rather than deterministic point estimates. Counterfactual analysis isolated the causal contributions of retrofit mechanisms and exposed saturation and synergy effects that would remain hidden in conventional finite element or fragility-based studies.

Collectively, these results establish that seismic resilience enhancement for the investigated tank is achieved not through isolated strengthening measures but through coordinated modification of interacting structural mechanisms. Effective retrofit requires simultaneous control of boundary degradation and shell instability sensitivity. For this specific configuration, hybrid integration provides a structural alignment with dominant failure pathways that neither confinement nor anchorage alone can achieve. Beyond structural response, the study clarified that retrofit success must be evaluated in terms of probabilistic damage evolution and operational impact rather than peak mechanical demand. Functional impairment likelihood, severe instability probability, and recovery burden emerged as more informative performance indicators for this tank than traditional stress- or displacement-based metrics. The hybrid retrofit consistently improved these resilience-oriented measures, particularly in regimes governing industrial risk.

In summary, this research demonstrated that the seismic behavior of the investigated petroleum storage tank is governed by uplift-driven boundary degradation coupled with shell-bottom junction instability, and that meaningful resilience gains are obtained only when retrofit strategies explicitly target both components of this coupled system. The hybrid retrofit framework introduced herein reshaped the structural–probabilistic response topology of the tank, reduced fragility curvature, compressed uncertainty, and enhanced robustness against extreme demand. These conclusions are specific to the studied reference tank and its uplift-sensitive shell–boundary configuration. Nevertheless, they provide a rigorous analytical basis for advancing from deterministic retrofit selection toward causally informed, uncertainty-aware resilience engineering for similar cylindrical storage systems.

Future research should focus on translating the abstract retrofit execution variables used in this study into constructible design specifications, integrating field monitoring data for digital twin updating, and extending the present framework to facility-level interactions among multiple tanks. Such developments would further strengthen the connection between advanced probabilistic analysis and practical industrial implementation. The present work establishes a methodological foundation for these efforts by demonstrating how nonlinear structural physics, Bayesian inference, and causal reasoning can be combined to deliver actionable, mechanism-resolved retrofit insights for uplift-sensitive petroleum storage tanks.

## 8. References

1. Abd-Elhamed, A., Slejko, E., & Cervone, A. (2025). Near-fault seismic assessment of cylindrical storage tanks. Journal of Risk and Reliability, 239(1).
2. Aghazadeh Dizaji, A. (2017). Buckling behavior of dented short cylindrical shells. Fen Bilimleri Enstitüsü.
3. Aghazadeh Dizaji, A. (2024a). Dynamic analysis of high-rise residential structures through the cone method. Edelweiss Applied Science and Technology, 8(6), 1895–1914.
4. Aghazadeh Dizaji, A. (2024b). Through what factors does polymer concrete have mechanical resistance? International Journal of Advanced Multidisciplinary Research and Studies, 4(6).
5. Aghazadeh Dizaji, A. (2024c). Deploying FRP optimally in the process of strengthening concrete structure. International Journal of Advanced Multidisciplinary Research and Studies.
6. Aghazadeh Dizaji, A., & Ahmadian, R. (2016). Transport corridors role in improving the urban environment studies. International Conference on Civil Engineering, Architecture and Cityscape.
7. Aghazadeh Dizaji, A., & Aydin, A. C. (2025). Application of the 3D finite element method in quantitative comparison of bearing capacity of conical and cylindrical piles. ISAR Journal of Science and Technology.
8. Aghazadeh Dizaji, A., & Aydın, A. C. (n.d.). Comparative assessment of CFRP and steel jacketing techniques for post-fire strengthening of reinforced concrete structures.
9. Aghazadeh Dizaji, A., Kiliç, M., Maali, M., & Aydin, A. C. (2023). Buckling behaviour of dented short cylindrical shells retrofitted with CFRP. Proceedings of the Institution of Civil Engineers - Structures and Buildings.
10. Alviz-Meza, A., Hadechini-Meza, F., & Perez, J. (2024). Deep learning classification of corrosion in above-ground storage tanks. Heliyon.
11. Aydin, A. C., Yaman, Z., Ağcakoca, E., Kiliç, M., Maali, M., & Aghazadeh Dizaji, A. (2020). CFRP effect on the buckling behavior of dented cylindrical shells. International Journal of Steel Structures, 20(2), 425–435.

12. Bajad, K. N., Jangid, R. S., & Patel, C. (2024). Performance of lead-rubber isolated liquid storage tanks with inertance. Journal of Risk and Uncertainty in Engineering Systems, Part A.
13. Bodenmann, L., Baker, J. W., & Stojadinović, B. (2024). Bayesian treatment of ground-motion uncertainty in fragility modeling. Earthquake Spectra.
14. Brunesi, E., Gabbianelli, G., & Nascimbene, R. (2025). Hydrodynamic pressure effects on metallic cylindrical tanks. Applied Sciences, 15(1), 474.
15. Celik, A. I., Demir, C., & Arslan, M. H. (2024). CFRP strengthening of cylindrical steel tanks under seismic loading. Journal of Computational Structural Engineering Institute of Korea.
16. Chen, B., Zhao, Y., & Wang, H. (2024). Digital twins for structural health monitoring of civil infrastructure. Smart Materials and Structures.
17. Chiappelloni, L., De Angelis, M., & Ciucci, M. (2025). Seismic effects on thin-walled atmospheric tanks via modal analysis. Engineering Proceedings, 85(1), 54.
18. Dehghan, S., Karimimansoob, V., Hoover, C. G., Sarabi, M. S., & Gheitarani, N. (2024a). Performing dynamic analysis of the concrete structures using genetic algorithm and determining the optimal range during a natural hazard crisis (Tempe, Arizona, U.S.A). International Journal of Advanced Multidisciplinary Research and Studies, 4.
19. Dehghan, S., Norouzian, M. M., Gheitarani, N., Heidarian, N., & Safaei-Mehr, M. (2024b). Application of geographic information system (GIS) for crisis management. International Journal of Advanced Multidisciplinary Research and Studies, 4.
20. Di-Sarno, L., Manfredi, G., & Prota, A. (2023). Seismic risk of petrochemical steel structures in aggressive environments. Bulletin of Earthquake Engineering.
21. Doustvandi, A., Tahamouli Roudsari, M., & Niazi, B. (2023). Seismic behavior of floating roof storage tanks with seals. Structural Durability & Health Monitoring, 17(1), 55–70.
22. Erkmen, B., Karalar, M., & Çavdar, Ö. (2024). Seismic performance assessment of anchored and self-anchored liquid storage tanks in high seismic regions. Bulletin of Earthquake Engineering, 22, 4197–4217.
23. Fang, S., Li, Y., & Zhou, Q. (2024). Bayesian hierarchical vulnerability assessment of large structures. Engineering Structures, 304, 117512.
24. Farrokhirad, E., & Gheitarani, N. (2024). Optimizing green wall strategies through public engagement. European Online Journal of Natural and Social Sciences, 13(2), 128–143.
25. Flaño, L., & Vallespín, J. (2024). Influence of geometric imperfections on seismic performance of slender tanks. International Journal of Pressure Vessels and Piping, 211, 105291.
26. Gabbianelli, G., Brunesi, E., & Nascimbene, R. (2025a). Near-field effects on seismic fragility of steel storage tanks. Infrastructures, 6(2), 24.
27. Gabbianelli, G., Brunesi, E., & Nascimbene, R. (2025b). Seismic fragility of tanks integrated in industrial frames. Soil Dynamics and Earthquake Engineering.
28. Ghadarjani, R., & Gheitarani, N. (2013). Public participation in rehabilitation of deteriorated housing. Haft Hesar Journal of Environmental Studies, 1(2), 75–83.
29. Ghadarjani, R., Gheitarani, N., & Khanian, M. (2013). Examination of city governorship pattern and citizen participation. European Online Journal of Natural and Social Sciences, 2(4), 601–608.
30. Gheitarani, N., Ghadarjani, R., Kahvand, M., & Mehrabadi, S. A. M. (2013a). Explaining effective measures in decreasing vulnerability of urban areas against earthquake using AHP model. Journal of Basic and Applied Scientific Research, 3(8), 675–681.
31. Gheitarani, N., Mosalsal, A., Rahmani, A., Khanian, M., & Mokhtari, M. (2013b). Urban design and vehicle–pedestrian conflict. World Applied Sciences Journal, 21(10), 1546–1551.
32. Gheitarani, N., Sara, E. S., Scott, C., Megha, B., Leah, G., & Mojtaba, K. (2020). Investigating the mechanism of place and community impact on quality of life of rural–urban migrants. International Journal of Community Well-Being, 3(1), 21–38.
33. Gheitarani, N., Sohrabi, S. A., Naghibi Iravani, S., & Dehghan, S. (2024a). Place attachment and quality of life. European Online Journal of Natural and Social Sciences, 13(1), 42–62.
34. Gheitarani, N., Sarabi, M. S., Sohrabi, S. A., & Dehghan, S. (2024b). Presenting a selected method for the industrial use of roller concrete through pavement. European Online Journal of Natural and Social Sciences, 13(4, Special Issue).
35. Gheitarani, N., Karimimansoob, V., Safaei-Mehr, M., & Norouzian, M. M. (2024c). Scrutinizing of city taxes effects on final housing price in Hamedan. European Online Journal of Natural and Social Sciences, 13(3), 235–245.
36. Gheitarani, N., & Norouzian, M. M. (2024d). Space configuration and identity of urban neighborhoods. European Online Journal of Natural and Social Sciences, 13(4).
37. Gheitarani, N. (n.d.). Spatial configuration as a method to measure the actual and potential ability of spaces used by indoor and outdoor users.
38. Hosseini, S., Hosseini, A., Gheitarani, N., & Samami, H. (2024). Artificial intelligence in conservation of Iranian architectural heritage.
39. Islam, N. U., & Jangid, R. S. (2024). Negative stiffness inerter dampers for seismic control of liquid tanks. Structures, 60, 105860.
40. Jayasinghe, S. C., Nguyen, T., & Zanganeh, H. (2024). Neural-network digital twins for real-time infrastructure monitoring. Ocean Engineering.
41. Jing, W., Feng, J., & Song, S. (2024). Seismic performance improvement of liquid storage tanks using base isolation and pendulum tuned mass dampers. Nuclear Engineering and Design, 417, 112867.
42. Jing, W., Feng, J., & Zhao, Y. (2024). Passive tuned mass dampers for seismic response reduction of liquid tanks. International Journal of Structural Stability and Dynamics, 24, 2450089.
43. Kahvand, M., Gheitarani, N., Khanian, M., & Ghadarjani, R. (2015). Urban solid waste landfill selection by SDSS: Case study Hamadan. Environment Protection Engineering, 41(2), 47–56.
44. Karimimansoob, V., Hoover, C. G., Sarabi, M. S., Gheitarani, N., & Sohrabi, S. A. (2024). Dynamic analysis of concrete structures using genetic algorithms. International Journal of Advanced Multidisciplinary Research and Studies, 4.
45. Karimimansoob, V., Safaei-Mehr, M., & Norouzian, M. M. (2024). City taxes and housing prices. European Online Journal of Natural and Social Sciences, 13(3), 235–245.
46. Khanian, M., Bolouhar, B., Gheitarani, N., & Nezhad, S. M. (2013). Studying the causes of vitality in traditional markets of Iran. World Applied Sciences Journal, 22(6), 831–835.
47. Khanian, M., Serpoush, B., & Gheitarani, N. (2019). Balance between place attachment and migration based on subjective adaptive capacity in response to climate change: The case of Famenin County in Western Iran. Climate and Development, 11(1), 69–82.

48. Lee, S. M., Yun, D. W., Park, D. U., & Jung, W. Y. (2024). Seismic fragility analysis of an anchored vertical gas storage tank using shaking-table testing. Advances in Mechanical Engineering, 16(2).
49. Li, W., Zhang, H., & Chen, Y. (2024). Evolution of digital twin research: A bibliometric analysis. Engineering Applications of Artificial Intelligence.
50. Li, X., Shan, W., & Wang, Y. (2025). Experimental study of soil–tank–liquid interaction in floating-roof tanks. Engineering Structures.
51. M. A. G., Norouzian, M. M., Gheitarani, N., Heidarian, N., & Safaei-Mehr, M. (2024). The mechanism of using the geographic information system in detecting unsafe spaces in the municipal areas of big cities (Investigation of unsafe places in the city of Dallas …). International Journal of Advanced Multidisciplinary Research and Studies, 4.
52. Maleki, E., Gheitarani, N., El-Sayed, S., Cloutier, S., & Giraud, G. (2024). Localized metric for estimating daylighting potential. International Journal of Ambient Energy, 45(1).
53. Men, J., Zhang, Y., Li, H., & Zhou, X. (2023). A hybrid deep belief network–based label distribution learning system for seismic damage probability of liquid storage tanks. Engineering Applications of Artificial Intelligence, 118, 105641.
54. Meng, X., Zhang, R., & Li, J. (2025). Seismic response of cylindrical tanks considering SSI and base isolation. Infrastructures, 10(6), 136.
55. Naghibi Iravani, S., Karimimansoob, V., Sohrabi, S. A., Gheitarani, N., et al. (2024a). Applying fuzzy logic and AHP in the design of residential spaces. European Online Journal of Natural and Social Sciences, 13(2), 144–160.
56. Naghibi Iravani, S., Sohrabi, S. A., Gheitarani, N., & Dehghan, S. (2024b). Spatial configuration as a method to measure space ability. European Online Journal of Natural and Social Sciences, 13(2), 90–104.
57. Naghibi Iravani, S., Sohrabi, S. A., Gheitarani, N., & Dehghan, S. (2024c). Planning methods for footpaths and sidewalks. European Online Journal of Natural and Social Sciences, 13(1), 1–20.
58. Naser, M. Z., & Tapeh, A. T. G. (2024). Causal inference for engineers: Concepts and applications. WIREs Data Mining and Knowledge Discovery, 14, e1533.
59. Norouzian, M. M., & Gheitarani, N. (2023). Impact of commercial sectors on environmental quality. International Journal of Advanced Multidisciplinary Research and Studies, 3.
60. Norouzian, M. M., & Gheitarani, N. (2025). Civil financial markets and environmental quality. Journal of Humanities and Education Development, 7(1).
61. Norouzian, M. M., & Guyadeen, D. (2025). Balanced scorecard method for municipal plans. Journal of Humanities and Education Development, 7(1).
62. Norouzian, M. M., Gheitarani, N., Heidarian, N., & Safaei-Mehr, M. (2024). GIS application for crisis management. International Journal of Advanced Multidisciplinary Research and Studies, 4.
63. Nosseir, A. E. S., Slejko, E. A., & Cervone, A. (2024). Composite tanks with embedded sensors for structural monitoring. Acta Astronautica.
64. Qurraie, S. S., & Gheitarani, N. (2025). Visual amenity of space. Multi Research Journal, 5(2).
65. Rahmat Rabi, R., Hoseini Vaez, S. R., & Kheyroddin, A. (2024). Probabilistic seismic vulnerability assessment of deformed ground-supported liquid storage tanks. Applied Sciences, 14(24), 11948.
66. Sadigh, S., Arash, S. S., Dehghan, S., & Gheitarani, N. (2023). Impact on seismic risk analysis of possible pulse in nearby areas. International Journal of Advanced Multidisciplinary Research and Studies, 3(6), 1560.
67. Samami, H., Naghibi Iravani, S., Sohrabi, S. A., Gheitarani, N., & Dehghan, S. (2024). Evaluation and optimization of building greening methods in four different climates using BIM. European Online Journal of Natural and Social Sciences, 13(1), 27–41.
68. Sarabi, M. S., Sohrabi, S. A., Dehghan, S., & Gheitarani, N. (2023). Impact of pulse-type motions on seismic risk. International Journal of Advanced Multidisciplinary Research and Studies, 3(6).
69. Sarabi, M. S., Sohrabi, S. A., Dehghan, S., & Gheitarani, N. (2024). Response mechanism of vertical concrete structures. International Journal of Advanced Multidisciplinary Research and Studies, 4.
70. Shan, W., Li, X., & Wang, Y. (2025). Uplift and soil–structure interaction effects on seismic response of unanchored cylindrical tanks. Journal of Constructional Steel Research, 226, 109235.
71. Shi, M., Zhang, J., & Chen, Z. (2025). Seismic performance of isolated liquid storage tanks with passive variable damping devices. Mechanical Systems and Signal Processing, 241, 113523.
72. Stoicescu, A. A., Ripeanu, R. G., & Toader, L. (2025). Multifactorial defect analysis of oil storage tanks. Processes, 13(8), 2575.
73. Tran, N. A., Nguyen, T., & Kim, D. (2025). Optimization of tuned liquid damping systems. Structure and Infrastructure Engineering.
74. Vasquez Munoz, L. E., & Dolšek, M. (2024). Parametric seismic fragility model for elephant-foot buckling in unanchored steel storage tanks. Bulletin of Earthquake Engineering, 22, 5775–5804.
75. Vasquez Munoz, L. E., Kramar, M., & Dolšek, M. (2024). Pushover-based seismic assessment of unanchored steel tanks with varying slenderness. Engineering Structures, 302, 117345.
76. Volikos, K., Konstandakopoulou, F., Asteris, P., & Hatzigeorgiou, G. (2025). Recent advances in seismic analysis of liquid storage tanks. Soil Dynamics and Earthquake Engineering, 198, 109309.
77. Wang, M., Sun, Z., Sun, J., Cui, L., Lyu, Y., & Wu, Y. (2023). Seismic fragility assessment of storage tanks considering different sources of uncertainty. Ocean Engineering, 283, 114972.
78. Wang, Z., Liu, Y., & Zhang, P. (2024). Tuned liquid mass dampers for low-frequency vibration control. Mechanical Systems and Signal Processing.
79. Zaker Haghighi, K., Gheitarani, N., Khanian, M., & Taghadosi, R. (2014). Examination of effects of urban street configuration on commercial buildings establishment. European Online Journal of Natural and Social Sciences, 3(1), 20–27.
80. Zakerhaghighi, K., Khanian, M., & Gheitarani, N. (2015). Subjective quality of life: Assessment of residents of informal settlements in Iran. Applied Research in Quality of Life, 10(3), 419–434.
81. Zhang, Y., Li, H., & Zhou, X. (2025). Uplift mechanics and annular baffles in unanchored tanks. Journal of Constructional Steel Research.